Multicolor and Spectral Characterization of Space Objects in the Near-IR

Eric C. Pearce[*], Harrison Krantz[*], Adam Block[*], Brad Sease[†], Mitchell Kirshner [‡], and Kris Rockowitz[*]

[*]*Steward Observatory, University of Arizona*

[†]*Computational Physics, Inc.*

[‡]*Systems and Industrial Engineering, University of Arizona*

ABSTRACT

The characterization of deep space debris poses a significant challenge in SSA. In order to be most useful, characterization should be performed quickly and under non-ideal observational conditions, generally using non-resolved techniques. The use of multi-color photometry and the resultant color indices potentially can rapidly discriminate between debris and intact space objects such as rocket bodies and satellites. However, these studies are not well informed by high resolution spectra of these same objects due to the lack of prior measurements with large astronomical telescopes.

During 2020 and early 2021, our team will measure an ensemble of rocket-bodies, intact spacecraft, and cataloged debris with both the UKIRT Wide Field Camera (WFCAM, 5-color near-IR photometry) and the UKIRT 1-5 μm Imager-Spectrometer (UIST). This data set will provide us with overlapping broadband IR colors and high-resolution spectra in the same color bands. Combined with previous WFCAM measurements in 2016-2017, and previous high-resolution visible band spectra with the MMT telescope, this is a unique data set. Our targets are carefully chosen to include a mix of objects with known compositions that will allow the development and evaluation of techniques to interpret our broadband near-IR photometry while being informed with the higher resolution spectra from UIST. The rocket bodies selected for study include the SL-12 fourth stage rocket bodies (SL-12 RB) measured in our previous 5-color survey. The intact payloads are chosen from satellites using the Boeing HS-376 busses. These objects' exteriors are dominated by solar panels which completely cover the spacecraft. Four different generations of solar panels were used over the twenty years of HS-376 development, with the earliest models using shallow function n/p silicon cells, and later models using GaAs/Ge single junction and GaInP2/GaAs/Ge dual junction panels. Both the SL-12 RB and Boeing HS-376 serve as ideal test objects of known composition for controlled studies. We will evaluate the efficacy of using near-IR color-indices to discriminate space debris and other objects from small solar-panel covered satellites.

In this paper, our team presents a prelude of our 2020-2021 observing campaign. The analyzed data, supplemented by our previous measurements with WFCAM and the MMT telescope, will be presented in a future paper.

1. INTRODUCTION

Since the launch of Sputnik in 1957, space surveillance has tracked and studied satellites and space debris with optical telescopes. The first attempts to use optical photometry to characterize satellites were published by the U.S and Russia in the late 1950s [1, 2]. The historical review papers by Lambert [3] and Sukhov [4] summarize much of the history of photometric technique development in the US and Russia respectively. Multi-color photometric measurements offer the opportunity to quickly assess the bulk spectral characteristics of a space object. The concept of exploiting the color indices in the visible bands has been previously explored in SSA. For example, BVRI photometry with the Cerro Tololo Inter-American Observatory (CTIO) 0.9 m telescope was used by Lederer et al. to compare measured color indices of 18 Initial Defense Communications Satellite Program (IDCSP) satellites with the predictions from laboratory measurements of solar cells [5].

We have studied the few published spectra of satellites on-orbit in the near-IR and found these wavelengths are highly diagnostic for satellite characterization. Two examples are the strong spectral features typically associated with solar cell band gaps in the 1.0–1.1 μm range (*c.f.* Figure 2 in [6]) and the strong features in the reflectance spectra of Kapton near 0.5 μm (c.f. Figure 3 in [7]) — both common satellite materials strongly influence red and near-IR color indices. The Z−Y and Z−J color indices are especially diagnostic of solar panel dominated space objects. In the visible part of the spectrum, the Sloan i' (695–844 nm), z_s[1] (826–920 nm), z' (> 820 nm), and Y (950–1058 nm) offer similar diagnostic features.

Few studies have focused on the efficacy of multi-color photometric characterization in the near-IR bands. One reason for this is that near-IR requires special cameras and large telescopes to achieve a comparable sensitivity to the visible bands. One study, conducted by D. Sanchez and his collaborators, measured 10 geosynchronous satellites in the J and H bands with the 3.6 m telescope at the Starfire Optical Range and an IR Laboratory NCMOS camera [8]. The study compared results to their own optical measurements and a comprehensive multicolor study by Beavers and Swezey that had high phase angle diversity [9]. Sanchez concluded that the near-IR observations are potentially more useful than visible band measurements for spectral characterization. Since both J and H are above typical solar panel band-gap features, Sanchez could not measure color indices across the solar cell band gap. Nonetheless, his photometric characterization showed encouraging results.

Previously we performed a study considering the efficacy of 5-color photometry in the near-IR to rapidly characterize geosynchronous space objects with the goal of distinguishing classes of objects and identifying anomalous members of classes [10]. The results were encouraging and showed that anomalous members could be identified from a class of objects. To date, our analysis of that data has focused on comparative analysis of SL-12 fourth stage rocket bodies as an ensemble of similar objects launched over several decades. At a later date we measured five of the previously observed SL-12 rocket bodies with the MMT telescope Blue Channel Spectrograph [11]. Consequently, we now have near-IR photometric measurements in five bands, visible band high resolution spectroscopy, and visible band multi-color high-speed photometry on the same set of objects (from our own instrument, Chimera).

Our intent is to use high-resolution spectroscopy to provide detailed insight into interpreting both near-IR and visible band photometry. We are scheduled in 2020 and early 2021 to perform new observations in the near-IR with both the UKIRT Wide Field Camera (WFCAM, 5-color near-IR photometry) and the UKIRT 1-5 μm Imager-Spectrometer (UIST). When completed we will have a complete set of photometry and spectroscopy in both the visible and near-IR bands on multiple SL-12 rocket bodies. In addition, we are targeting observations of solar panel covered Boeing HS-376 satellites which similarly make up an ensemble of similar objects launched over a twenty-year period. Our previous results show that old solar panel covered spacecraft were easily discriminated using color indices. Frith and his colleagues at NASA JSC published a similar study using 5-color near-IR photometry to study an ensemble of inactive solar panel covered Boeing HS-376 satellites using many of the same concepts [12]. However, none of these previous studies were well informed by high resolution spectral data on the same objects that could aid in the interpretation of the multi-color photometry.

2. SELECTED TARGET OBJECTS

For our observations we focus on two groups of objects: SL-12 rocket bodies and HS-376 satellite busses. Both consist of ensembles of like objects which were launched in modest number over a period of twenty or more years. During this time there were modifications and developments to each design, but both remained largely unchanged. We can observe an individual object and compare measurements against other objects of the same population. Through this method we expect to identify anomalous members, identify changes with design, and changes associated with on-orbit aging.

---

[1] Here z_s refers to the Astrodon filter which cuts off the open-ended Sloan z at 920 nm.

2.1 SL-12 FOURTH STAGE ROCKET BODY

The SL-12 (also called the "Proton K") was a mainstay Russian four-stage to GEO launch vehicle that was used from 1974 (see Figure 1) [13, 14]. The SL-12 fourth stage rocket bodies (henceforth referred to as "SL-12 RB") offer a convenient ensemble of objects for which photometric techniques can be developed and tested. The rocket bodies are bright (11.5 mag in the Z band, or 12 m_v), and at least 25 such objects are available within the longitude range visible from Hawaii and Tucson, Arizona. This upper stage inserted the payload into GEO from its transfer orbit and discarded itself in GEO without moving to a graveyard orbit.

The SL-12 RB had at least three different versions. The Blok DM (1974) and Blok DM-2 (1982) were similar in structure and fuel but differed slightly in length. A third version (DM-2M) was developed specifically to support sea launches and is structurally similar to the DM-2. The SL-12 RB is large, measuring 3.7 m in diameter and approximately 6.2 m long (the DM-2 version). Reportedly the fourth stage could impart a rotation rate of up to 1.5 rpm for spacecraft separation, although observed rotational spin rates of discarded SL-12 rocket bodies are typically significantly faster (5–12 rpm).

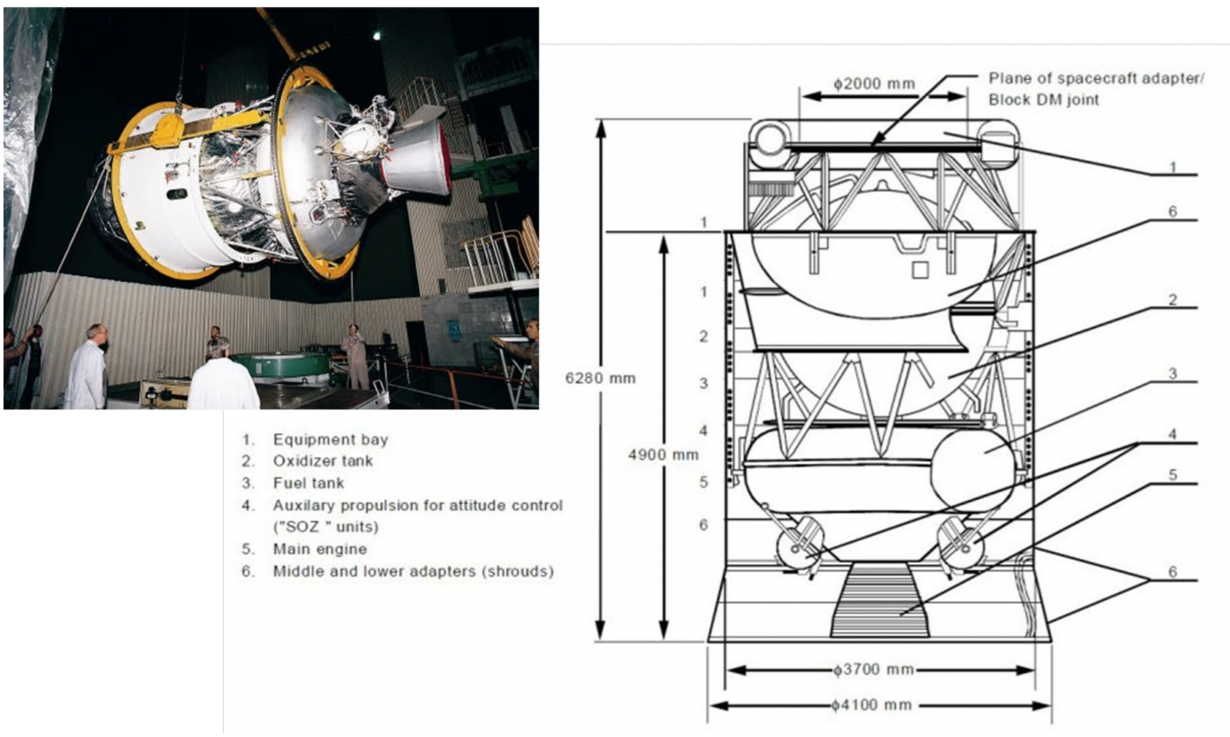

Figure 1. Photograph and line drawing of the SL-12 fourth stage rocket body.

2.2 BOEING HS-376 SATELLITE BUS

The HS-376 satellite bus was a common communications satellite bus with a total of 58 launched from 1978 to 2003 [15], many of which are observable from the Hawaii and Tucson observatory locations. The satellite bus features a cylindrical body with two sections, one of which nests inside the other and extends outward in orbit (see Figure 2). The cylindrical body is 2.2 m in diameter and extends to between 6.5 m and 7 m long. The exterior surface is almost completely covered in solar cells and is otherwise largely featureless. The main body of the spacecraft is spin-stabilized at 50 rpm and the payload shelf despun to provide radio antenna pointing. An antenna reflector unfolds from the end of the satellite bus. At end-of-life the spin-rate is no longer maintained and the despun section becomes coupled with the rest of the satellite. The transfer of inertia from the body to the previously despun mass results in a reduction of the overall spin rate compared to the operational spin rate.

There were four major variations to the design of the HS-376: the standard HS-376, the long-life HS-376L, the higher-powered HS-376HP, and the larger HS-376W. Only the HS-376W featured a notably different bus with a larger diameter cylindrical body. Only four of the HS-376W were launched. During the twenty-year evolution of the HS-376, the solar cell technology was incrementally upgraded for new satellites. Four different generations of solar cells were used: the earliest HS-376 busses used shallow function n/p silicon cells while later models used GaAs/Ge single junction and GaInP2/GaAs/Ge dual junction panels. Reflectance spectra for only two of these four generations of solar cells have been published in the open literature.

Firth et. al. have previously measured a selection of these objects with UKIRT and documented phase angle variation on the J-K and H-K color indices. Phase angle variations in J-K and H-K of order 0.2 to 0.3 magnitudes were observed, and although the satellites shared some common trends, each displayed its own unique characteristic [12].

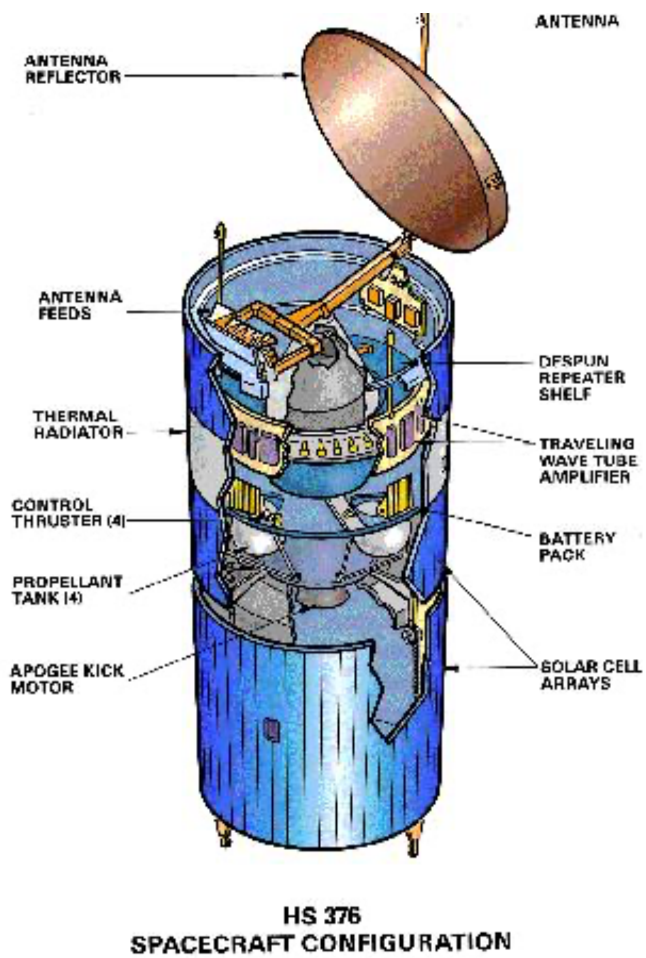

Figure 2. Drawing of the standard HS-376 satellite bus.

3. PREVIOUS MEASUREMENTS AND OBSERVATIONS

We previously conducted observations with multiple different telescopes and instruments. In 2016-2017 we made near-IR photometric measurements with UKIRT WFCAM. In 2019 we made visible band spectroscopic measurements with the MMT telescope Blue Channel Spectrograph. Starting in 2018 we have made semi-regular visible band measurements with Chimera, a high-speed three-color photometer on the Steward Observatory Kuiper telescope.

3.1 UKIRT WFCAM NEAR-IR PHOTOMETRY

The 3.8 m United Kingdom Infra-Red Telescope (UKIRT) is the largest dedicated IR telescope located on Mauna Kea in Hawaii. The telescope has a suite of astronomical spectrographs and imagers operating at the Cassegrain focus, and a unique large mosaic near-IR survey camera (Wide Field CAMera; WFCAM) that operates at the prime focus [16]. The UKIRT control system features a robust queue scheduler and allows data collection on satellites using standard two-line element sets (TLEs).

During late 2016 and early 2017 we conducted a near-IR 5-color survey of a suite of space objects [10]. This survey included 55 separate data collections on 24 unique SL-12 RBs that were launched from 1977 to 2012. Examples of both major variants were included in the sample (12 DMs, 12 DM-2s). Figure 3 shows a typical five-color collection on one of the SL-12 RB in our sample, 1987-109D (SCN 18718), an original Blok DM. This collection was our original long ZYJHK observing protocol which cycled through each filter over approximately 39 minutes. Typical integration times were 5 seconds in Z, Y, J, and H, and 10 seconds in K. The typical sensitivity of WFCAM is 19.1 (Z), 18.7 (Y), 18.1 (J), 17.3 (H), 16.7 (K) in 5 seconds at a signal-to-noise ratio (SNR) of 5. The longer collection time in the K band is a consequence of our early interest in the K band for potential thermal emission during eclipse. Later collections used a quicker 15-minute sequence.

Although the details of the collection protocols evolved during the survey, most collections initially acquired the space object near the center of camera 3 in the Z band, then sequenced through the near IR filters Z, Y, J, H and K. The sequences started with the Z band to maximize detection sensitivity for the initial acquisition. Later protocols shortened the sequence significantly and finished the sequence with a brief second collection in Z band to provide both astrometric calibration and a photometric reference that could be compared back to the beginning of the track. A typical data collection sequence would take between 10 and 40 minutes.

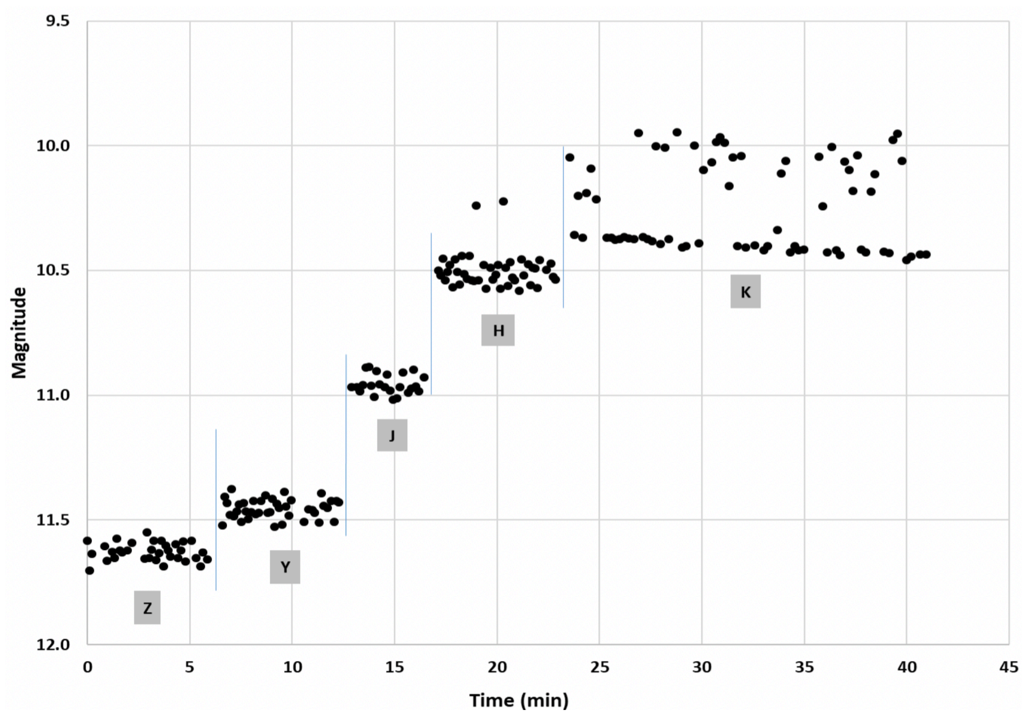

Figure 3. Typical WFCAM survey 5-color collection on an SL-12 RB. The scatter in the Z-H band is due to aliasing between the integration time and rotational period of the satellite. The bright features in K band were commonly observed in the SL-12 signatures and is unexplained.

3.2 MMT VISIBLE BAND SPECTRA

The MMT is a 6.5 m multi-purpose telescope located on Mount Hopkins south of Tucson Arizona [17]. The MMT Spectrograph is a two-channel low-intermediate resolution echelle spectrograph originally commissioned with the MMT telescope in 1979 and later upgraded with new detectors [18, 19]. The original design paralleled the Hale Double Spectrograph's dual optical paths, one optimized for the blue end of the visible spectrum, and the other for red, optimized for the spectral response of detectors in the late 1970s. For our measurements, only the blue channel was available [2], providing a spectral coverage of 520 nm range at a dispersion of 0.196 nm/pixel.

In 2019 we recorded spectra of five SL-12 RBs selected from the list of those previously observed with UKIRT [11]. The large collecting aperture of the MMT allowed the rapid collection of multiple high SNR spectra with short 2-minute exposures. These short exposures enabled the rapid collection of many high-quality spectra in the limited time available for the observations. Additionally, solar phase angle changes during the integration were minimal. Furthermore, since typical rotational periods of SL-12 RBs are 5-15 seconds, the effects of rotation are averaged out. Figure 4 shows one example spectrum.

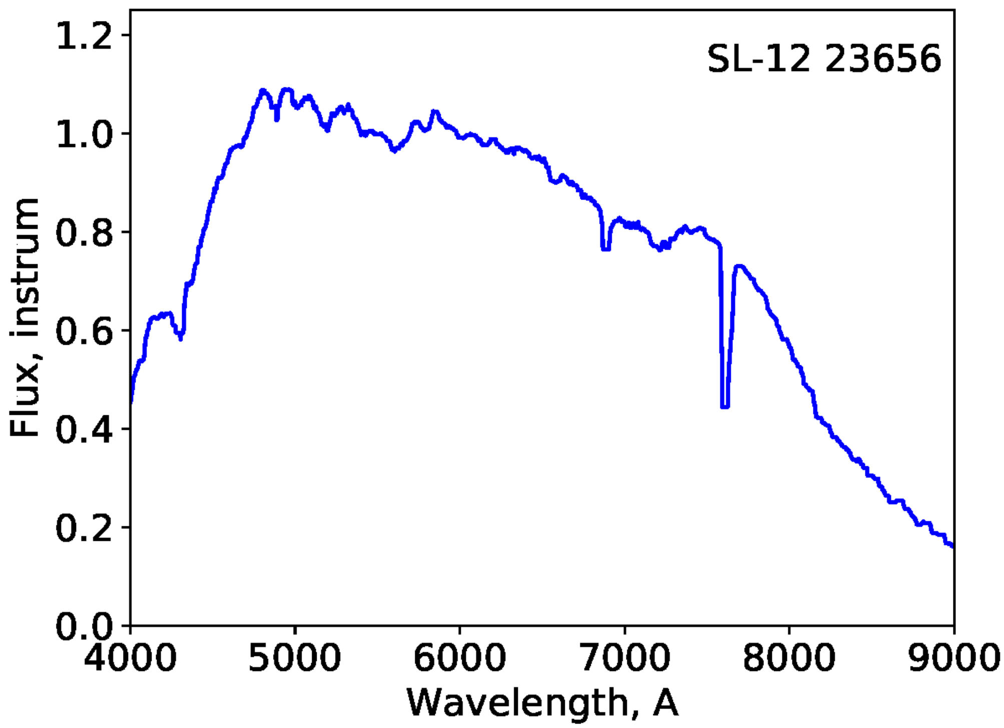

Figure 4. Spectrum of 1995-045D (SSC 23656), the youngest SL-12 RB in the sample.

The five SL-12 RBs measured represent a span of on-orbit ages from 23 to 35 years. For comparison we normalized the spectra of each rocket body against the youngest. Figure 5 shows this comparison and demonstrates a trend that the older SL-12 RB are less reflective in the red, an effect of on-orbit aging.

[2] During these measurements, a high-speed EM-CCD camera was mounted at the normal location of the Red Channel Dewar and was performing time critical observations for another satellite observing program. Consequently, the phase angle and elevation of the SL-12 RB collections were opportunistic.

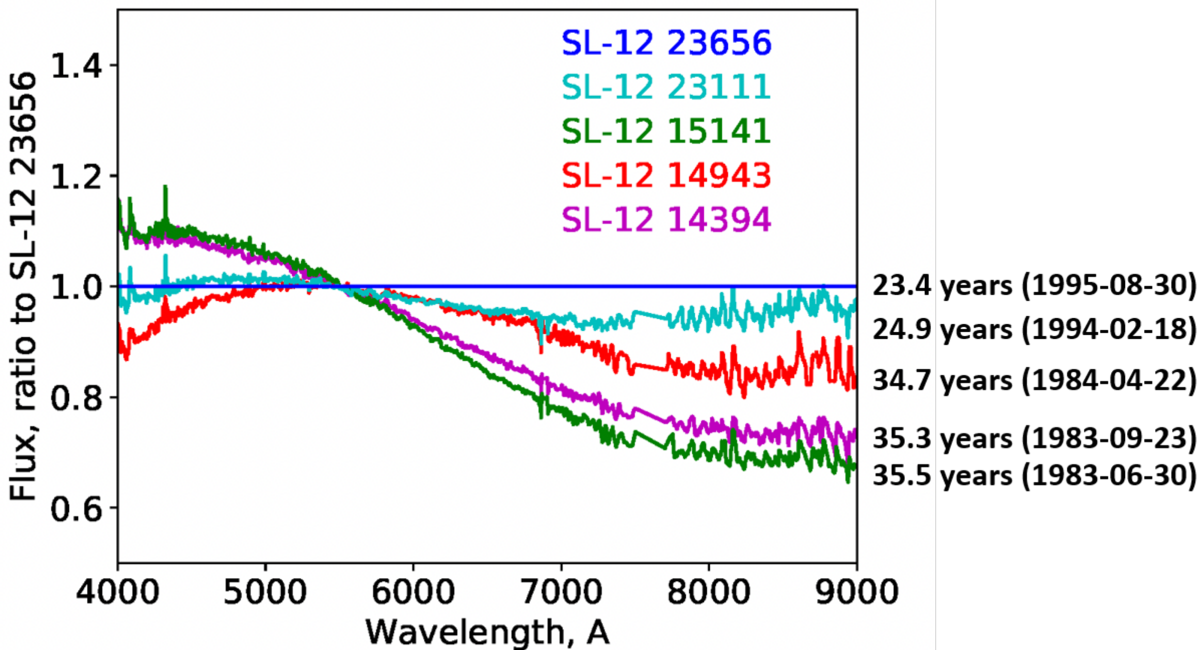

Figure 5. Comparison of the spectra of the five SL-12 upper stage RBs. All spectra have been normalized to the youngest RB, 1995-045D (23656).

3.3 CHIMERA HIGH-SPEED VISIBLE BAND PHOTOMETRY

Chimera is a high-speed EMCCD-based three-color photometer for space surveillance and astronomy. Chimera has three Princeton EMCCD cameras which simultaneously observe the Sloan r’, i’, and z’ color bands [20]. Designed specifically for space surveillance, Chimera records photometry with time resolution up to hundreds of frames per second. This speed combined with the simultaneous multicolor capability can differentiate reflections and characterize the motion and structure of satellites. Moreover, utilization of color-indices from the simultaneous imaging, instead of absolute photometry, greatly simplifies calibration and enables use of this technique under a broad range of operational conditions. The Chimera instrument is optimized for use on the Steward Observatory 1.55 m Kuiper Telescope located on Mount Bigelow, and is routinely used for various SSA and astronomical observing programs [21].

The unique abilities of Chimera allow the sampling of a spacecraft light curve at a high time resolution which enables the characterization of the rotational period and sub-period features. The three cameras of Chimera, each observing a different color band, are synchronized such that all three cameras trigger and expose simultaneously. The light curve of each color band can be unambiguously compared, and any time dependent color difference revealed.

The SL-12 RBs observed by Chimera thus far exhibit a range of rotational periods of 5-15 seconds (see an example light curve in Figure 6), consistent with the observations of other researchers [22,23]. Through examination of the light curve and correlation with the diagrams and images of the SL-12 RB one can guess the structural elements which produce specular reflections. Time dependent color differences in the reflections may be related to material usage and aging-related changes. Additionally, documenting the rotational periods will provide valuable information for accompanying observations including those described in this paper.

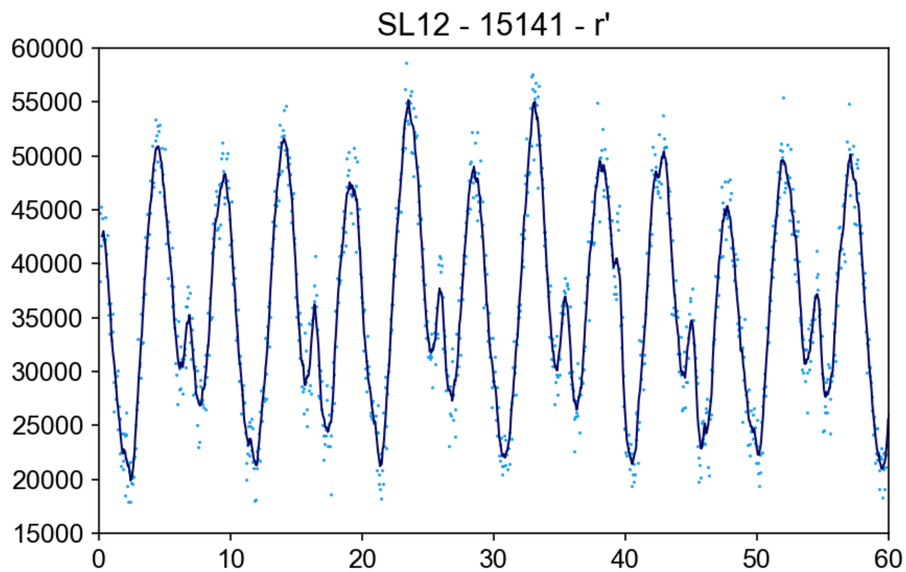

Figure 6. Light curve of SL-12 RB 1983-066F (15141) from the Chimera photometer (Sloan r', 50 ms integration times, ~20 fps).

In addition to the SL-12 RBs, we have used Chimera to survey several HS-376 satellites. The satellites observed all exhibit similar light curves with rotational periods in the 3-4 second range (see Figure 7), corresponding to 15-20 rpm, much slower than the operational spin-stabilized 50 rpm. Each rotation is characterized by four specular flashes of different brightness and shape. These reflections are likely from the flat antenna reflector which extends from the end of the cylindrical body.

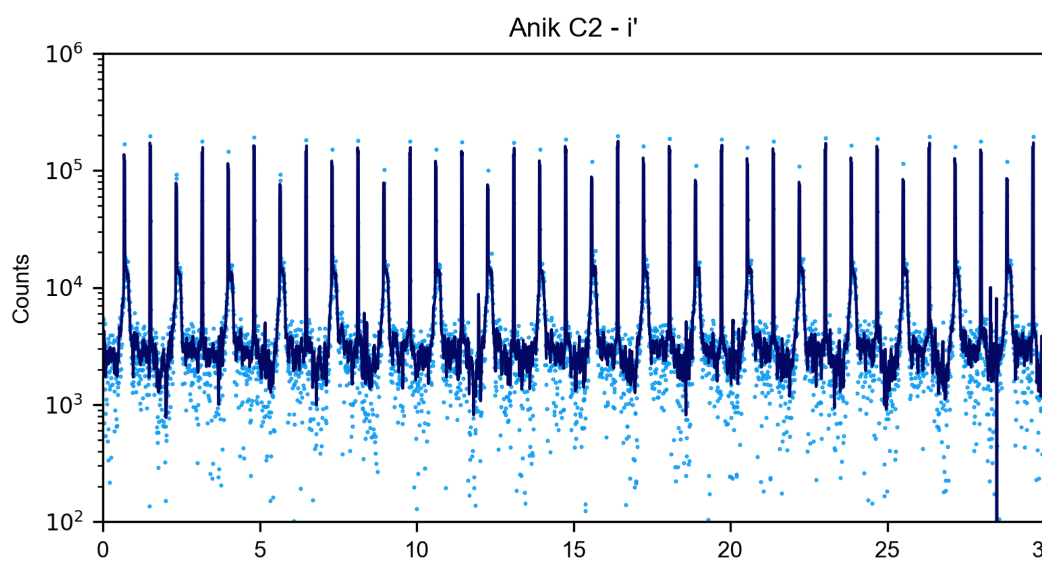

Figure 7. Light curve of HS-376 based satellite Anik C2 from the Chimera photometer (Sloan i', 5.7 ms integrations times, ~174 fps).

4. UPCOMING OBSERVATIONS

During 2020 and early 2021, our team will measure an ensemble of rocket-bodies, intact spacecraft, and cataloged debris with both the UKIRT WFCAM (5-color near-IR photometry) and the UKIRT 1-5 μm Imager-Spectrometer (UIST). Our targets, including the SL-12 RB and Boeing HS-376 satellite bus, are carefully chosen to include a mix of objects with known compositions that will allow the development and evaluation of techniques to interpret our broadband near-IR photometry while being informed with the higher resolution spectra from UIST. This comprehensive data set will provide us with overlapping broadband IR colors, and high-resolution spectra in the same color bands. Combined with previous WFCAM measurements in 2016-2017 and previous high-resolution visible band spectra with the MMT telescope, this is a unique data set.

Based on our previous study, there are two significant challenges in the interpretation of near-IR photometric colors for satellite characterization using WFCAM. First, we need a measurement protocol that balances the desire for unambiguous instantaneous color indices and time series photometry while reducing the overhead of the WFCAM filter changes. Our previous observations stressed time series photometry in each color band and minimized filter changes. Second, we must account for the rotational variation of the object. While this problem is inherent with any non-simultaneous photometric technique, the longer integration times required in the near-IR make this problem more cumbersome. Typical WFCAM integration times are approximately the same as typical rotational periods and the individual frames are slightly irregular in spacing. We must be careful to ensure that individual measurements accurately measure a rotationally averaged intensity and consider aliasing in our interpretation of the light curves.

While full time resolved near-IR photometry and spectrometry could be of significant value, neither is possible with a reasonable SNR with the apertures provided by the UKIRT telescope. Consequently, we supplement our measurements with separately observed simultaneous multi-color optical photometry from the Chimera high-speed photometer. Optical photometry produces time resolved signatures and rotational rates to inform the interpretation of the WFCAM near-IR signatures and to confirm our expectation that the spectra measurements are rotationally averaged.

5. INTENTIONS AND EXPECTATIONS

For our upcoming observations we plan to utilize a new scheduling method to focus on color index measurements while accounting for overhead time lost to filter changes. We plan to densely sample the photometric and spectral observations over the entire range of available phase angle for each collection period. Our goal with this data is to develop methods of analysis for broadband photometry which are informed by accompanying high-resolution spectra. Our future observations of SL-12 RBs and HS-376 satellites with both near-IR photometry and spectra, combined with our previous measurements in the visible band, will produce a comprehensive data set for this research.

We expect these techniques will demonstrate that near-IR photometric measurements can clearly discriminate space debris from solar-panel featured satellites. Our review of previous measurements shows color variation as a function of phase angle, particularly for the HS-376 satellites. Additionally, the different generations of satellites may be identified based on the solar cell technology and resultant band gaps in the spectra.

6. ACKNOWLEDGEMENTS

This work was funded by the United States Naval Observatory in support of its ongoing research into dynamics and characterization of near Earth and Solar System objects, and by the University of Arizona Office of Research, Discovery and Innovation.

Observations reported here were obtained at the MMT Observatory, a joint facility of the University of Arizona and the Smithsonian Institution.

Observations reported here were obtained with the Kuiper 61” Telescope operated by the University of Arizona Steward Observatory. The Chimera Photometer was developed with funding the University of Arizona Office of Research, Discovery and Innovation.

7. REFERENCES

1. J. G. Moore, "Photometric Observations of the Second Soviet Satellite (1957 β1)," *Publications of the Astronomical Society of the Pacific*, vol. 71, (419), pp. 163–165, 1959.

2. V. M. Grigorevskij, "About Methods of Photometry of Artificial Earth's Satellites," Byulleten' Stantsii Nablyudenia ISZ, No. 7, p. 14, 1959.

3. J. V. Lambert and K.E. Kissell, "The Early Development of Satellite Characterization Capabilities at the Air Force Laboratories," in *Proceedings AMOS Conference*, Wailea, Maui, Hawaii, 2006.

4. P. P. Sukhov and K. P. Sukhov, "On some problems of photometric identification of geostationary satellites," Kinematics and Physics of Celestial Bodies, vol. 31, (6), pp. 314–318, 2015.

5. S.M. Lederer *et al*, "Preliminary Characterization of IDCSP Spacecrafts through a Multi-Analytical Approach," in *Proceedings AMOS Conference*, Wailea, Maui, Hawaii, 2012.

6. K. J. Abercromby, P. Abell, and E. Baker, "Reflectance Spectra Comparison of Orbital Debris, Intact Spacecraft, and Intact Rocket Bodies in the GEO Regime," *Fifth European Conference on Space Debris*, Darmstadt, Germany, 2009.

7. L. Bai *et al*, "Spectral Scattering Characteristics of Space Target in Near-UV to Visible Bands," *Optical Express* vol. 22, (7), pp. 8515–8524, 2014.

8. D.J. Sanchez et al. (2000), "Photometric Measurements of Deep Space Satellites," *Proceeding of SPIE*, International Symposium on Optical Science and Technology, San Diego CA, 31 October 2000.

9. W.I. Beavers and L.W. Swezey (1995), "Optical Monitoring of Geosynchronous Satellites, Final Report." MIT Lincoln Laboratory Project Report STK-240, October 1995.

10. E.C. Pearce *et al.* (2017), "Rapid Characterization of Geosynchronous Space Debris with 5-Color Near-IR Photometry," *Proceedings AMOS Conference*, Maui HI, September 2017.

11. E. C. Pearce *et al.* (2020), "Examining the effects of on-orbit aging of SL-12 rocket bodies using visible band spectra with the MMT," *Journal of Space Safety Engineering*, 2020.

12. J. Frith, P. Anz-Meador, S. Lederer, H. Cowardin, and B. Buckalew (2015), "NIR Color vs Launch Date: A 20-year Analysis of Space Weathering Effects on the Boeing 376 Spacecraft," *Proceedings AMOS Conference*, Maui HI, September 2017.

13. "Mission Overview GE-6 Launch on the Proton Launch Vehicle," International Launch Services, 2000.

14. Gunter's Space Page, "Blok-D," available: http://space.skyrocket.de/doc_stage/blok-d.htm, 2020.

15. Gunter's Space Page, "Hughes/Boeing: HS-376/BSS-376," available: https://space.skyrocket.de/doc_sat/hs-376.htm, 2020.

16. M. Casali *et al*, "The UKIRT Wide-field Camera," *Astronomy and Astrophysics*, vol. 467, (2), pp. 777-784, 2007.

17. W.G. Grant (2018), "The MMT Observatory: Entering a New Era of Scientific Discovery," *Proceedings of the SPIE*, Ground-based and Airborne Telescopes VII, Vol. 10700, id. 107002T, 6 July 2018.

18. J.R.P. Angel, R.L Hilliard, and R.J. Weymann (1979), SAO Special Report, ed. T. Weekes, No. 385, p. 87.

19. G.D. Schmidt, R.H. Weymann, and C.B. Foltz (1989), "A Moderate-Resolution, High-Throughput CCD Channel for the Multiple Mirror Telescope Spectrograph," *Publications Astronomical Society of the Pacific*, Vol. 101, pp. 713–724, August 1989.

20. H. Krantz, E.C. Pearce, L. Avner, O. Durney, C. Sauve, C. (2018). “Chimera: A high-speed three-color photometer for space surveillance and astronomy,” *Proceedings of the SPIE, Astronomical Telescopes and Instrumentation*, Austin TX, 6 July 2018.

21. University of Arizona (2019), “Kuiper 61” Telescope”, https://www.as.arizona.edu/kuiper-61-telescope, downloaded 14 August 2019.

22. V. S. Yurasov, V. G. Vygon, and V.D. Shargorodskiy, "Classification and Identification of Geostationary Space Objects by Using Coordinate and Photometric Observations,” in *Proceedings of the Sixth US/Russian Space Surveillance Workshop*, Russian Academy of Science, St. Petersburg, Russia, 2005.

23. T. Cardona et al. (2016), “BVRI Photometric Observations and Light-Curve Analysis of GEO Objects,” *Advances in Space Research,* v. 58, pp 514–527.